Self-healing of Gaussian and Bessel beams: a critical comparison

Andrea Aiello[1,2*] and Girish S. Agarwal[3]

[1] *Max Planck Institute for the Science of Light,*

Günther-Scharowsky-Strasse 1/Bau24, 91058 Erlangen, Germany

[2]*Institute for Optics, Information and Photonics, University of Erlangen-Nuernberg,*

Staudtstrasse 7/B2, 91058 Erlangen, Germany and

[3] *Department of Physics, Oklahoma State University, Stillwater, Oklahoma 74078, USA*

(Dated: January 26, 2015)

Abstract

Contrarily to a common belief, any beam of light possesses to a some extent the ability to "reconstruct itself" after hitting an obstacle. The celebrated Arago spot phenomenon is nothing but a manifestation of this property. In this work we analyze the self-healing mechanism from both a mathematical and a physical point of view, eventually finding a new expression for the minimum reconstruction distance, which is valid for *any* kind of beam, including Gaussian ones. Finally, a witness function that quantify the self-reconstruction capability of a beam is proposed and tested. The results presented here help clarifying the physics underlying self-healing mechanism in optical beams.

* andrea.aiello@mpl.mpg.de

I. INTRODUCTION

In this paper we illustrate, with the help of several examples, the self-healing property exhibited by different types of optical beams. In particular, we analyze and compare the behavior of Gaussian, Bessel, Bessel-Gauss beams and of a pair of plane waves. In recent years, the remarkable capacity of a beam to reconstruct itself after encountering an obstacle (self-healing mechanism) attracted considerable interest and has been the subject of numerous theoretical and experimental investigations [1–7]. In this context, particularly relevant is the theoretical work by Chu and coworkers [8, 9].

The aim of this work is to study further the self-reconstruction ability possessed by different kind of light beams, thus extending our previous work on this subject [10]. For all the *scalar* beams studied here, we model the obstacle as a soft-edge aperture with a Gaussian profile, in order to be able to produce formulas in closed form. In particular, after a careful analysis of the self-healing mechanism from a mathematical and physical point of view, we can find a new expression for the minimum reconstruction distance z_{min}. Then, a witness function that quantifies the similarity between the field of the unperturbed beam (namely, the beam that would propagate as if the obstacle were not present) and the field of the perturbed one (that is, the beam that propagates behind the obstruction), is proposed and tested. Finally, our findings are illustrated by means of a quantitative comparison between the self-healing properties of a Gauss beam and a Bessel beam. The notation utilized throughout this paper is given in Appendix A.

II. SELF-HEALING AND THE EIGENVALUE PROBLEM

A. Basic definitions and formal developments

Consider a scalar field $f(x, y, z)$ propagating along the z-axis. An obstruction, characterized by a given amplitude transmission function $t_O(x, y)$, is placed in the plane $z = 0$. The amplitude $f_O(x, y, 0)$ of the obstructed field in the plane $z = 0$ can be written as

$$f_O(x, y, 0) = t_O(x, y)f(x, y, 0). \tag{1}$$

According to the definition of angular spectrum, the amplitude $f_O(x, y, z)$ of the field transmitted at distance z from the obstruction can be written as

$$f_O(x, y, z) = \frac{1}{2\pi} \iint\limits_{-\infty}^{\infty} F_O(k_x, k_y) \exp\left[i\left(xk_x + yk_y + zk_z\right)\right] dk_x dk_y, \tag{2}$$

2

where $k_z = (k^2 - \kappa^2)^{1/2}$, with $\kappa^2 = k_x^2 + k_y^2$ and $F_O(k_x, k_y) = \mathcal{F}\left[f(x,y,0)t_O(x,y)\right](k_x, k_y)$, namely

$$F_O(k_x, k_y) = \frac{1}{2\pi} \int\!\!\!\int_{-\infty}^{\infty} f(x,y,0)t_O(x,y) \exp\left[-i\left(xk_x + yk_y\right)\right] dxdy$$

$$= \frac{1}{2\pi} \int\!\!\!\int_{-\infty}^{\infty} \left[\int\!\!\!\int_{-\infty}^{\infty} F(\vec{\kappa}')\, e^{i\vec{\rho}\cdot\vec{\kappa}'} \frac{d^2\kappa'}{2\pi}\right]\left[\int\!\!\!\int_{-\infty}^{\infty} T_O(\vec{\kappa}'')\, e^{i\vec{\rho}\cdot\vec{\kappa}''} \frac{d^2\kappa''}{2\pi}\right] e^{-i\vec{\rho}\cdot\vec{\kappa}}\, dxdy$$

$$= \frac{1}{2\pi} \int\!\!\!\int_{-\infty}^{\infty} d^2\kappa' \left\{ F(\vec{\kappa}') \int\!\!\!\int_{-\infty}^{\infty} d^2\kappa'' \left[T_O(\vec{\kappa}'') \int\!\!\!\int_{-\infty}^{\infty} e^{i\vec{\rho}\cdot(\vec{\kappa}'+\vec{\kappa}''-\vec{\kappa})} \frac{dxdy}{(2\pi)^2} \right]\right\}$$

$$= \frac{1}{2\pi} \int\!\!\!\int_{-\infty}^{\infty} F(\vec{\kappa}')T_O(\vec{\kappa} - \vec{\kappa}')d^2\kappa', \tag{3}$$

where $d^2\kappa = d\kappa_x d\kappa_y$, $d^2\kappa' = d\kappa'_x d\kappa'_y$, et cetera. The final expression for $f_O(x,y,z)$ is thus given by

$$f_O(x,y,z) = \frac{1}{(2\pi)^2} \int\!\!\!\int_{-\infty}^{\infty} \exp\left(i\vec{\rho}\cdot\vec{\kappa}\right) \exp\left(izk_z\right) \left[\int\!\!\!\int_{-\infty}^{\infty} T_O(\vec{\kappa} - \vec{\kappa}')F(\vec{\kappa}')\, d^2\kappa'\right] d^2\kappa. \tag{4}$$

Given the function $t_O(x,y)$, one can always define the transmission function $t_A(x,y)$ of an aperture *complementary* to the obstruction via the relation (Babinet principle)

$$t_A(x,y) + t_O(x,y) = 1. \tag{5}$$

By definition, both $t_A(x,y)$ and $t_O(x,y)$ are non-negative real-valued functions. Using this equation into Eq. (1) yields to

$$f_O(x,y,0) = \left[1 - t_A(x,y)\right]f(x,y,0)$$
$$= f(x,y,0) - t_A(x,y)f(x,y,0)$$
$$\equiv f(x,y,0) - f_A(x,y,0). \tag{6}$$

Substituting Eq. (6) into Eq. (4) one obtains

$$f_O(x,y,z) = \frac{1}{(2\pi)^2} \int\!\!\!\int_{-\infty}^{\infty} \exp\left(i\vec{\rho}\cdot\vec{\kappa}\right) \exp\left(izk_z\right) \Bigg[$$

$$\times F(\vec{\kappa}) - \int\!\!\!\int_{-\infty}^{\infty} T_A(\vec{\kappa} - \vec{\kappa}')F(\vec{\kappa}')\, d^2\kappa'\Bigg] d^2\kappa$$

$$\equiv f(x,y,z) - f_A(x,y,z), \tag{7}$$

where $T_A(\vec{\kappa}) = \mathcal{F}[t_A](k_x, k_y)$ and the definition of the "transmitted" function $f_A(x, y, z)$ is obvious. Taking the absolute value squared of both sides of either Eq. (6) or Eq. (7) (the integrals are anyway independent from z) and integrating over the *whole* xy-plane, we obtain

$$\overline{I}(f_O) = \overline{I}(f - f_A)$$

$$= \overline{I}(f) + \overline{I}(f_A) - 2\operatorname{Re} \int\!\!\!\int\limits_{-\infty}^{\infty} f^*(x, y, 0) f_A(x, y, 0)\, dxdy, \tag{8}$$

where the average beam intensity $\overline{I}(h)$ is defined as

$$\overline{I}(h) = \int\!\!\!\int\limits_{-\infty}^{\infty} h^*(x, y, z) h(x, y, z)\, dxdy. \tag{9}$$

Equation (8) already shows that *perfect* self-healing is impossible even in principle because the intensity of the transmitted field is unavoidably reduced unless $\overline{I}(f_A) = 0$.

B. Defining self-healing

An optical beam is dubbed "self-reconstructing" when has the ability to recover its initial amplitude or intensity profile after interaction with an obstacle. This means that the field of a self-reconstructing beam is expected to obey the law

$$f_O(x, y, z) \approx \lambda_0 f(x, y, z), \tag{10}$$

for $z \geq z_0$, where z_0 denotes the so-called *minimum reconstruction distance* and the scaling factor $\lambda_0 = \left[\overline{I}(f_O)/\overline{I}(f)\right]^{1/2}$ accounts for the average intensity reduction caused by the interaction with the obstruction. The left side of Eq. (10) is given by Eq. (4), while the right side can be written as

$$\lambda_0 f(x, y, z) = \frac{\lambda_0}{2\pi} \int\!\!\!\int\limits_{-\infty}^{\infty} F(k_x, k_y) \exp\left[i\left(xk_x + yk_y + zk_z\right)\right] dk_x dk_y$$

$$= \frac{1}{2\pi} \int\!\!\!\int\limits_{-\infty}^{\infty} \exp\left(i\vec{\rho} \cdot \vec{\kappa}\right) \exp\left(izk_z\right) \left[\lambda_0 F(\vec{\kappa})\right] d^2\kappa. \tag{11}$$

Substituting Eqs. (4) and (11) into (10), we obtain the following simple relation:

$$F_O(\vec{\kappa}) \approx \lambda_0 F(\vec{\kappa}), \tag{12}$$

where Eq. (3) has been used.

It is crucial to notice that Eq. (12) *does not* contain the variable z while, conversely, the relation (10) is supposed to be true only for $z \geq z_0$. The latter requirement cannot be

ignored because by definition Eq. (10) cannot be satisfied at $z = 0$ where, instead, Eq. (6) must be fulfilled. Hence, we are apparently faced with a paradox here. In fact, Eq. (12) constitutes more a statement about the obstruction rather than the field. This can be seen by using Eq. (11) to rewrite (12) in the more suggestive form

$$\frac{1}{2\pi} \int\!\!\!\int_{-\infty}^{\infty} T_O(\vec{\kappa} - \vec{\kappa}') F(\vec{\kappa}')\, d^2\kappa' \approx \lambda_0 F(\vec{\kappa}). \tag{13}$$

If we replace the approximation symbol "$\approx$" with the equality one "$=$" in Eq. (13), then the latter takes the form of a *homogeneous Fredholm integral equation of the second kind* [11] with the unknown function $F(\vec{\kappa})$, which has to be an eigenfunction, associated with the eigenvalue λ_0, of the integral kernel $T_O(\vec{\kappa} - \vec{\kappa}')$ describing the obstruction. This means that the requirement (10) is indeed too much restrictive because it can be satisfied only by those beams whose angular spectrum (the eigenfunction) is unaffected by the interaction with the obstruction, apart from a trivial proportionality factor (the eigenvalue), as shown in Eq. (13).
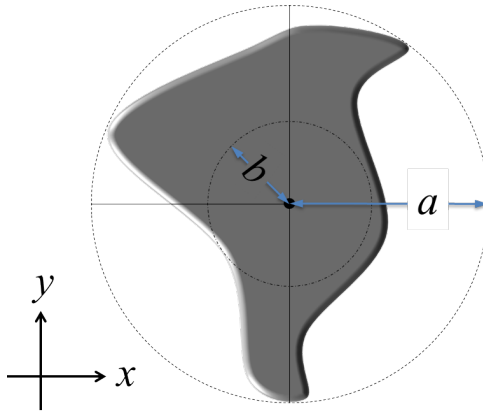

FIG. 1.   The orthogonal projection of the obstruction on the xy-plane is represented by the dark-gray area. This region is circumscribed by the dashed circle of radius a (circumradius) and it inscribes the dot-dashed circle of radius b (inradius). Both circles are centered along the z-axis of the beam at $x = 0 = y$.

C.   Redefining the minimum reconstruction distance

Key to the apparent paradox illustrated above, is the existence of the minimum reconstruction distance z_0 after which a self-reconstructing beam restores its initial profile. For a single plane wave $\exp(i\vec{k} \cdot \vec{r})$ with wave vector $\vec{k} = k\,(\hat{x} \sin\theta \cos\phi + \hat{y} \sin\theta \sin\phi + \hat{z} \cos\theta)$, this parameter can be straightforwardly determined in the context of either geometrical and wave optics [10]. Consider an obstruction whose orthogonal projection on the xy-plane

occupies an area O, and let a be the *radius* (circumradius) of the circle inside which such projection can be inscribed and centered on the axis of the beam (see Fig. 1 above). Then z_0 can be estimated as

$$z_0 \propto \frac{a}{\tan \theta}, \tag{14}$$

where the proportionality factor essentially depends on the shape of the obstruction. However, a beam of light can always be thought as a bunch of plane waves whose density in the k-space is determined by the absolute value squared $|F(k_x, k_y)|^2$ of the angular spectrum of the field $f(x, y, z)$ representing the beam. Moreover, given the wave vector $\vec{k} = k(\hat{x} \sin \theta \cos \phi + \hat{y} \sin \theta \sin \phi + \hat{z} \cos \theta) = \hat{x} k_x + \hat{y} k_y + \hat{z} k_z$, it is evidently possible to rewrite

$$\begin{aligned}
\frac{1}{\tan \theta} &= \frac{k_z}{\left(k_x^2 + k_y^2\right)^{1/2}} \\
&= \frac{\left(k^2 - k_x^2 - k_y^2\right)^{1/2}}{\left(k_x^2 + k_y^2\right)^{1/2}},
\end{aligned} \tag{15}$$

provided that $k_x^2 + k_y^2 \leq k^2$. This condition is necessary to maintain k_z real-valued and it limits the applicability of the equation above to beams whose angular spectrum does not contain evanescent waves [12]. From Eq. (15) it follows that we can regard the expression of z_0 given in Eq. (14) as a function of $\kappa = (k_x^2 + k_y^2)^{1/2}$ in the k-space, namely

$$z_0 \rightarrow a\, Z(\kappa) = a\, \frac{\left(k^2 - \kappa^2\right)^{1/2}}{\kappa}. \tag{16}$$

On account of the fact that the transverse wave vector $\vec{\kappa}$ has a density distribution function $|F(k_x, k_y)|^2$, we (arbitrarily) *define* the minimum reconstruction distance z_0 as the *expected value* of the function $a\, Z(\kappa)$, namely

$$\frac{z_0}{a} = \langle Z(\kappa) \rangle = \frac{\displaystyle\iint\limits_{k_x^2+k_y^2 \leq k^2} \frac{\left(k^2 - \kappa^2\right)^{1/2}}{\kappa} |F(\vec{\kappa})|^2 \, d^2\kappa}{\displaystyle\iint\limits_{k_x^2+k_y^2 \leq k^2} |F(\vec{\kappa})|^2 \, d^2\kappa}, \tag{17}$$

where both integrals are limited to the disk of equation $k_x^2 + k_y^2 \leq k^2$. It is convenient to express the integrals in Eq. (17) in cylindrical coordinates $k_x = \kappa \cos \varphi$, $k_y = \kappa \sin \varphi$ to

6

obtain

$$
\begin{aligned}
\frac{z_0}{a} &= \frac{\displaystyle\int_0^{2\pi} d\varphi \int_0^1 ds\, \left(1 - s^2\right)^{1/2} \mathcal{F}(s, \varphi)}{\displaystyle\int_0^{2\pi} d\varphi \int_0^1 ds\, s\, \mathcal{F}(s, \varphi)} \\[2em]
&= \frac{\displaystyle\int_0^{2\pi} d\varphi \int_0^{\pi/2} d\theta\, \cos^2\theta\, \mathcal{F}(\sin\theta, \varphi)}{\displaystyle\int_0^{2\pi} d\varphi \int_0^{\pi/2} d\theta\, \sin\theta \cos\theta\, \mathcal{F}(\sin\theta, \varphi)},
\end{aligned}
\tag{18}
$$

where we have defined $s = \kappa/k = \sin\theta$ and $\mathcal{F}(s, \varphi) = |F(\kappa\cos\varphi, \kappa\sin\varphi)|^2$.

In the remainder of this section, we check the validity of Eq. (18) for the cases of *1.* a *fundamental Gaussian beam* and *2.* a *Bessel-Gauss beam*; both obstructed by a soft-edge Gaussian aperture. For the sake of clarity in the following examples we shall restrict our attention to the paraxial regime of propagation.

1. Fundamental Gaussian beam

Consider the transmission of a fundamental Gaussian beam of waist w_0 across a soft-edge Gaussian obstacle of full width $2a$ located along the axis of the beam at $z = 0$. The obstruction is described by the transmission function

$$
t_O(x, y) = 1 - \exp\left(-\frac{|\vec{\rho} - \vec{\rho}_0|^2}{2a^2}\right),
\tag{19}
$$

where $\vec{\rho}_0 = \hat{x}x_0 + \hat{y}y_0$ represents the displacement of the obstacle with respect to the beam propagation axis. A straightforward calculation gives

$$
T_O(k_x, k_y) = 2\pi\delta\left(\vec{\kappa}\right) - a^2 \exp\left(-i\,\vec{\kappa} \cdot \vec{\rho}_0\right) \exp\left[-\frac{a^2}{2}\left(k_x^2 + k_y^2\right)\right].
\tag{20}
$$

The field describing the Gaussian beam can be written as $f(x, y, z) = \exp\left(ikz\right) g(x, y, z)$, with $g(x, y, z)$ being the fundamental solution of the paraxial wave equation

$$
g(x, y, z) = \frac{1}{z - iz_R} \exp\left[i\frac{k}{2}\left(\frac{x^2 + y^2}{z - iz_R}\right)\right],
\tag{21}
$$

and $z_R = kw_0^2/2$ denotes the Rayleigh range. The Fourier transform at $z = 0$ of this field can be easily calculated and the result is

$$
G(k_x, k_y) = \frac{i}{k} \exp\left[-\frac{z_R}{2k}\left(k_x^2 + k_y^2\right)\right].
\tag{22}
$$

7

From Eqs. (3,21-22) and a straightforward Gaussian integration, we obtain

$$G_A(k_x, k_y) = \frac{ia^2}{a^2 k + z_R} \exp\left[-\frac{k}{2}\frac{|\vec{\rho}_0|^2}{a^2 k + z_R} - i\vec{\kappa}\cdot\vec{\rho}_0 \frac{z_R}{a^2 k + z_R}\right] \exp\left(-\frac{a^2}{2}\frac{k_x^2 + k_y^2}{a^2 k + z_R}\right), \quad (23)$$

with, by definition, $G_O(k_x, k_y) = G(k_x, k_y) - G_A(k_x, k_y)$. Using this result into Eq. (2) yields to the following expression for the beam transmitted beyond the obstacle:

$$g_A(x, y, z) = \frac{a_R}{z_R}\frac{1}{z - ia_R} \exp\left[i\frac{k}{2}\left(\frac{x^2 + y^2}{z - ia_R}\right)\right], \quad (24)$$

where, for the sake of clarity, we have chosen $\vec{\rho}_0 = \vec{0}$ and we have defined the modified Rayleigh range a_R of the beam $g_A(x, y, z)$ transmitted by the aperture complementary to the obstruction, as

$$a_R = \frac{z_R}{1 + \dfrac{z_R}{ka^2}} \leq z_R. \quad (25)$$

The self-healing capability of a fundamental Gaussian beam is vividly illustrated in Fig. 2.
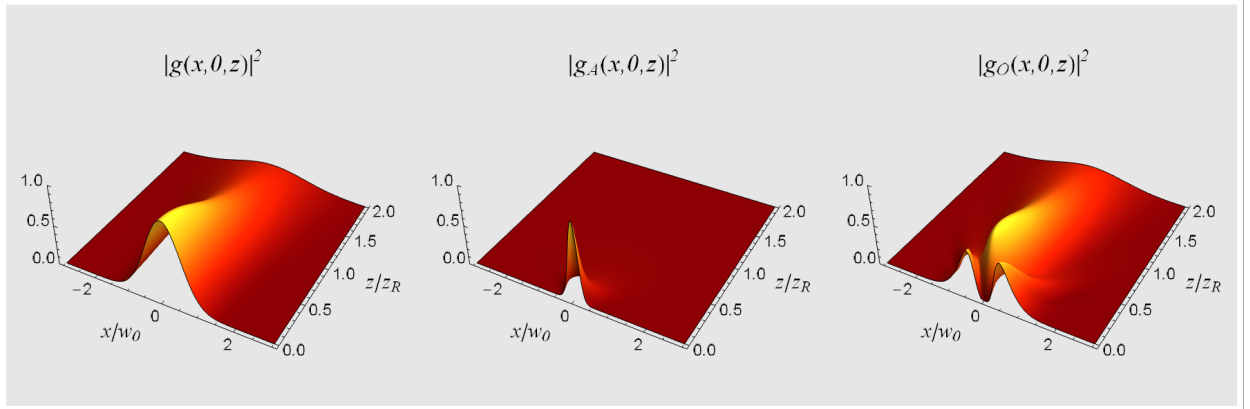

FIG. 2. Plots of the intensity distributions (absolute value squared) evaluated at $y = 0$, of (left to right): the incident field $g(x, 0, z)$, the "virtual" field transmitted by the aperture complementary to the obstruction $g_A(x, 0, z)$, and the field transmitted behind the obstacle $g_O(x, 0, z)$. The plots are generated for a Gaussian beam with angular aperture $\theta_0 = 2/(kw_0) = \pi/12 \sim 15°$ and a soft-edge Gaussian obstruction with full width $a/w_0 = 0.2$ and $x_0 = 0 = y_0$. At $z/z_R = 2$ the intensity profiles of the fields $g(x, 0, z)$ and $g_O(x, 0, z)$ appear very similar.

A close inspection of this figure together with Eqs. (24-25) reveals how the mechanism underlying the self-reconstruction process works. From Eq. (25) it follows that $a_R \leq z_R$. Ergo, the "virtual" field $g_A(x, y, z)$ transmitted by the complementary aperture spreads in the xy-plane, while propagating along the z-axis, much more rapidly than the unperturbed field $g(x, y, z)$. Therefore, for $z \gtrsim 2$ the intensity profile of the obstructed beam almost coincides with the profile of the unperturbed one. This process is depicted in Fig. 3 where
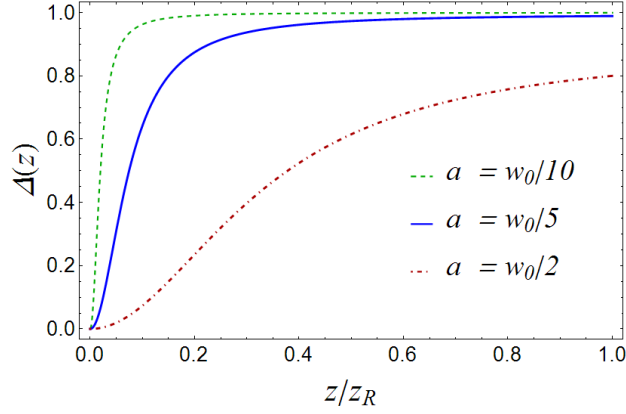
8

the normalized difference $\Delta(z)$ of the *on-axis* field intensities $I(0,0,z) = |g(0,0,z)|^2$ and $I_A(0,0,z) = |g_A(0,0,z)|^2$ is plotted as function of z/z_R:

$$\Delta(z) = \frac{I(0,0,z) - I_A(0,0,z)}{I(0,0,z)}. \tag{26}$$

From Eq. (22) it follows that $\mathcal{F}(s,\varphi) = |G(\kappa\cos\varphi, \kappa\sin\varphi)|^2 = \exp\left(-2s^2/\theta_0^2\right)$, where

FIG. 3. Plots of the the normalized difference $\Delta(z)$ of the *on-axis* field intensities $I(0,0,z) = |g(0,0,z)|^2$ and $I_A(0,0,z) = |g_A(0,0,z)|^2$. For long propagation distances $z \gg z_R$ the asymptotic value is $\Delta(\infty) = 1 - (a_R/z_R)^2 = (1 + 4\alpha^2)/(1 + 2\alpha^2)^2$, where $\alpha \equiv a/w_0$.

$\theta_0 = 2/(kw_0)$ denotes the so-called *angular spread* of the Gaussian beam [12]. Using this result in Eq. (18) yields to

$$\frac{z_0}{a} = \frac{\pi}{2\theta_0^2} \frac{\mathrm{I}_0(1/\theta_0^2) + \mathrm{I}_1(1/\theta_0^2)}{\sinh\left(1/\theta_0^2\right)} \tag{27}$$

$$\approx \frac{(2\pi)^{1/2}}{\theta_0} \frac{1}{1 - \exp\left(-2/\theta_0^2\right)}, \qquad (\theta_0 \ll 1),$$

where $\mathrm{I}_\nu(z)$ denotes the *modified Bessel function of the first kind* of order ν [13]. A plot of z_0/a is given in Fig. 4 a). Since for $\theta_0 \ll 1$ it has $\theta_0 \approx \tan\theta_0$, then in the paraxial regime of propagation

$$\frac{z_0}{a} \approx \frac{(2\pi)^{1/2}}{\tan\theta_0}, \qquad (\theta_0 \ll 1), \tag{28}$$

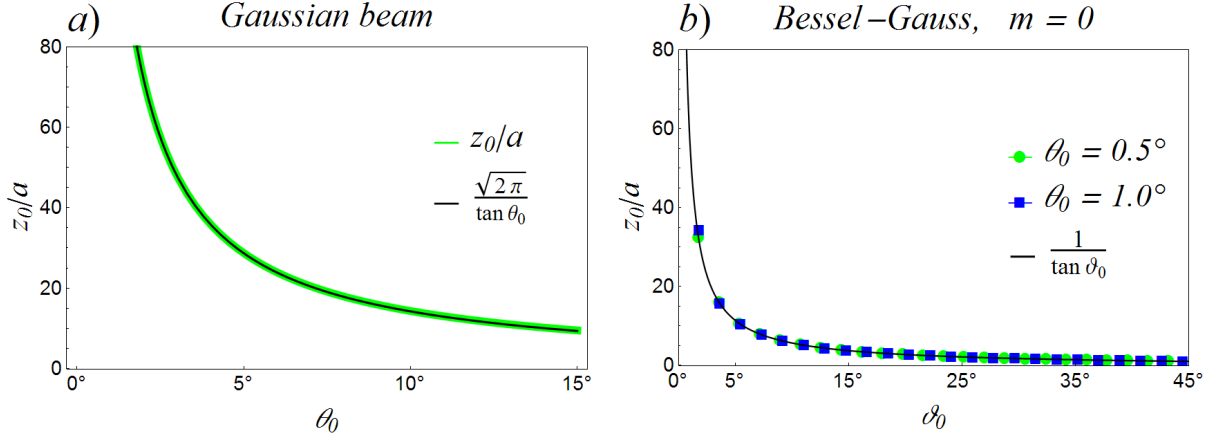which is consistent with the expected geometrical optics result.

9

FIG. 4. Plots of the minimum reconstruction distance z_0/a as given in Eq. (18), evaluated for *a*) a Gaussian beam and *b*) a zeroth-order ($m = 0$) Bessel-Gauss beam. *a*) Plot of Eq. (27) (green line) compared with the modified geometrical-optics value (black line). *b*) Scatter plots of numerically integrated Eq. (18) with $\mathcal{F}(s, \varphi)$ given by Eq. (31) for different angular spreads θ_0 of the Gaussian envelope. Green circles: $\theta_0 = 0.5°$; blue squares: $\theta_0 = 1.0°$. The black line represents the "one-over-tangent" geometrical-optics prediction and is presented for comparison.

2. Bessel-Gauss beam

Consider a Bessel-Gauss beam transmitted across the same soft-edge Gaussian obstruction as above. The field describing such beam can be written in $z = 0$ as

$$f(x, y, 0) = (\pm 1)^m \exp\left(\pm im\phi\right) J_m(\kappa_0 \rho) \exp\left(-\frac{\rho^2}{w_0^2}\right), \qquad (m = 0, 1, 2, \cdots), \qquad (29)$$

where $\rho = (x^2 + y^2)^{1/2}$, $\kappa_0 = k \sin \vartheta_0$ and $J_\nu(z)$ denotes the Bessel function of the first kind of order ν [13]. The two key parameters characterizing the beam are the aperture ϑ_0 of the Bessel cone in k-space, and the waist w_0 (or, equivalently, the angular spread $\theta_0 = 2/(kw_0)$) of the Gaussian envelope. The Fourier transform at $z = 0$ of this field is given, for $m \geq 0$, by the following expression:

$$F(k_x, k_y) = \frac{w_0^2}{2\, i^m} \exp\left(\pm im\varphi\right) I_m\left(\frac{\kappa\, \kappa_0}{2/w_0^2}\right) \exp\left(-\frac{\kappa^2 + \kappa_0^2}{4/w_0^2}\right). \qquad (30)$$

Taking the absolute value squared of the function above yields to

$$\mathcal{F}(s, \varphi) = I_m^2\left(s\, \frac{2 \sin \vartheta_0}{\theta_0^2}\right) \exp\left[-\frac{2}{\theta_0^2}\left(s^2 + \sin^2 \vartheta_0\right)\right]. \qquad (31)$$

In this case the integrals in Eq. (18) cannot be calculated analytically and a numerical evaluation of the latter is necessary. The resulting values of z_0/a are portrayed in Fig. 4 *b*) as functions of the aperture ϑ_0, non necessarily paraxial, of the Bessel cone.

10

For $\theta_0 \ll 1$ the Bessel-Gauss beam reduces to an ordinary Bessel beam. In such a limit we recover the expected geometrical optics result:

$$\frac{z_0}{a} \approx \frac{1}{\tan \vartheta_0}, \qquad (\theta_0 \ll 1). \tag{32}$$

The two examples shown in this section show that Eq. (17) furnishes an appropriate measure of the minimum reconstruction distance z_0.

III. RESOLUTION OF THE PARADOX

In this section we seek a solution for the paradox outlined earlier. The conundrum may be stated as follows: How is it possible to obtain the simultaneous validity of both Eq. (1) and Eq. (10)? In mathematical terms, the problem amounts to understand if and how it is possible achieve both

$$f_O(x,y,0) = t_O(x,y)f(x,y,0) \qquad \text{AND} \qquad f_O(x,y,z) \approx \lambda_0 f(x,y,z) \qquad \forall z \geq z_0. \tag{33}$$

As it will be clear soon, the solution of this problem is closely connected to the question raised by Chu&Wen [9] about how to quantify the similarity between the two functions $f_O(x,y,z)$ and $f(x,y,z)$ in order to describe the self-reconstruction ability of a beam. The reader is addressed to Appendix B for a shortly review of the Chu&Wen approach.

A. Similarity as relative distance

Let us begin our discussion about similarity between functions by illustrating a simple, prototypical example of a self-reconstructing beam. Consider a "skeleton" Bessel beam made of two plane waves only, with wave vectors lying on the xz-plane and forming the angles ϑ_0 and $-\vartheta_0$, respectively, with the z-axis. Let $f(x,y,z)$ be the complex-valued scalar field representing such a "beam" for $z \leq 0$:

$$f(x,y,z) = \frac{1}{2}\exp\left(ikz\cos\vartheta_0\right)\left[\exp\left(ikx\sin\vartheta_0\right) + \exp\left(-ikx\sin\vartheta_0\right)\right]. \tag{34}$$

This beam hits at $z = 0$ a semitransparent obstacle described by the Gaussian transmission function (19) that here we rewrite as

$$t_O(x,y) = 1 - \exp\left[-\frac{(x^2 - x_0)^2 + (y - y_0)^2}{2a^2}\right], \tag{35}$$

with $a > 0$. The field $f_O(x,y,z)$ transmitted beyond the obstacle at $z > 0$ can be straightforwardly calculated and the expression is

$$f_O(x,y,z) = \frac{1}{1 + iz/(ka^2)}\exp\left[-\frac{1}{2a^2}\frac{(x - x_0)^2 + (y - y_0)^2}{1 + iz/(ka^2)}\right]\exp\left[-i\frac{k\sin^2\vartheta_0}{2}\frac{z}{1 + iz/(ka^2)}\right]$$
$$\times \cos\left[k\sin\vartheta_0\frac{x + ix_0 z/(ka^2)}{1 + iz/(ka^2)}\right]. \tag{36}$$

It is easy to verify that, as expected,

$$\lim_{a\to\infty} f_O(x,y,0) = f(x,y,0). \tag{37}$$

The "virtual" field $f_A(x,y,z)$ transmitted by the aperture complementary to the obstacle can be obtained from the relation

$$f(x,y,z) = f_O(x,y,z) + f_A(x,y,z). \tag{38}$$

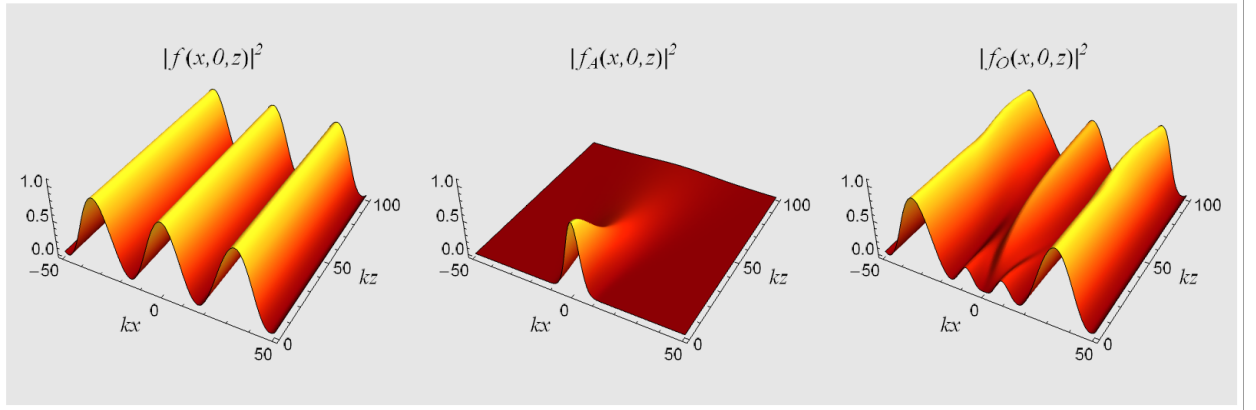The absolute value squared of the three fields f, f_A and f_O is shown in Fig. 5 below.

FIG. 5.   Plots of the intensity distributions (absolute value squared) evaluated at $y = 0$, of (left to right): the original field $f(x,y,z)$, the "virtual" field transmitted by the aperture complementary to the obstruction $f_A(x,0,z)$, and the field transmitted behind the obstruction $f_O(x,y,z)$. The plots are generated with $\vartheta_0 = \pi/32 \sim 6°$, $ka = 5$ and $x_0 = 0 = y_0$. For these values the geometrically predicted minimum reconstruction distance is equal to $z_0 = 2^{1/2}a/\tan\vartheta_0 \sim 72/k$. At $kz = 100$ the intensities of the fields $f(x,y,z)$ and $f_O(x,y,z)$ appear already very similar.

From this figure it is evident the "self-healing mechanism" in action: during propagation from $z = 0$, where the obstacle is located, to $kz = 100$ the field practically recovers its original intensity distribution. However, it should be noticed that due to the finite transverse extent of the obstruction, the intensity $I_O(x,0,z) = |f_O(x,0,z)|^2$ changes considerably during propagation only within the region $|kx| \lesssim 30$. Conversely, it remains constantly close to $I(x,0,z) = |f(x,0,z)|^2$ in the complementary region $|kx| \gtrsim 30$. This phenomenon appears more clearly if one displays in the same figure the three intensity distributions at different z, as shown in Fig. 6 next page.

This means that for all practical purposes Eq. (10) represents a far too much restrictive constraint. What one really needs is simply to satisfy (10) on the xy-plane in the neighborhood of the propagation axis z. This statement may be formalized as follows. Consider again an obstruction whose orthogonal projection on the xy-plane occupies the region O, and let E be an arbitrary area in the xy-plane *strictly* contained within O, namely $E \subset O$.
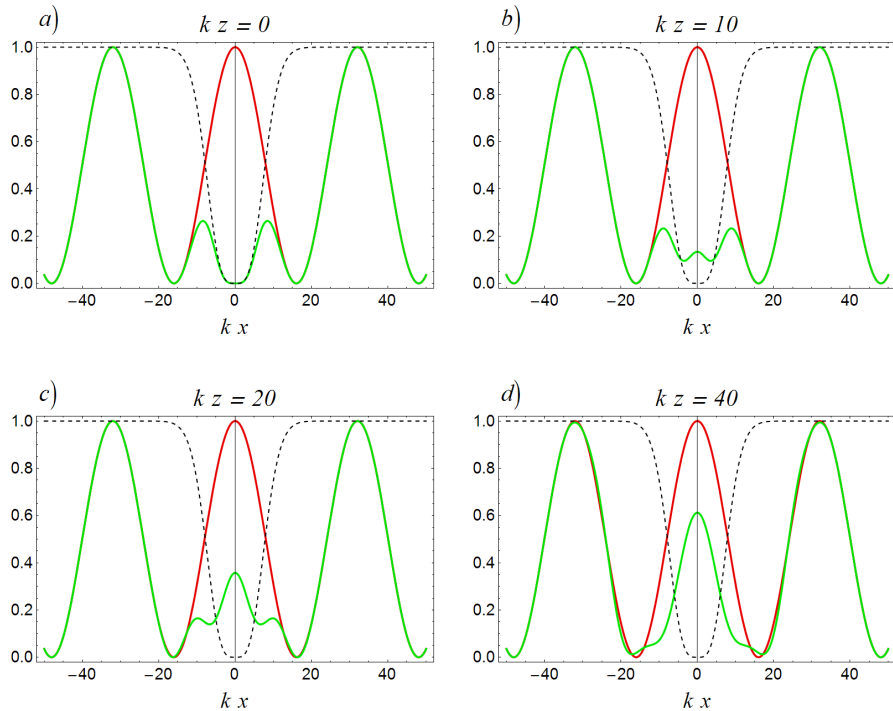
12

FIG. 6. Intensity distributions $I(x, y, z) = |f(x, y, z)|^2$ (red lines) and $I_O(x, y, z) = |f_O(x, y, z)|^2$ (green lines) evaluated at $y = 0$ and a) $z = 0$, b) $kz = 10$, c) $kz = 20$ and d) $kz = 40$. The black dashed curves represent the intensity transmission function $|t_O(x, y)|^2$ evaluated at $y = 0$. The values of the parameters A_0, ϑ_0, a, x_0 and y_0 are the same as in Fig. 4. It is evident how at *any* $z \geq 0$ it has $I_O(x, 0, z) \simeq I(x, 0, z)$ for $k|x| \gtrsim 30 = 6ka$.

For example, E can be the region confined by the inner circle of radius b in Fig. 1. Then, as necessary condition for self-haling, we require that the amplitude $f_O(x, y, z)$ of the obstructed beam is proportional to the amplitude $f(x, y, z)$ of the unperturbed beam *only* within E:

$$f_O(x, y, z)\Big|_{(x,y)\in E} \approx \lambda_0 f(x, y, z)\Big|_{(x,y)\in E} \qquad \forall z \geq z_0. \qquad (39)$$

From a mathematical point of view, Eq. (39) makes much more sense than Eq. (10). In fact, according to the theory of *angular spectrum representation* of a beam [12], the field configuration at $z = 0$ completely determines the field distribution at $z > 0$. Therefore, if at a certain distance z Eq. (10) were satisfied upon *all* the xy-plane, then it should be also valid at $z = 0$. But the latter statement is clearly false because at $z = 0$ one has, by definition,

$$f_O(x, y, 0) = t_O(x, y) f(x, y, z) \neq f(x, y, z). \qquad (40)$$

Thus, we have shown that the origin of the apparent paradox (33) resides in the desideratum of satisfying both equations (1) and (10) over all the xy-plane. This is also the reason why

the similarity defined in equation (1) of Ref. [9], fails to furnish a quantitative description of self-healing: The double integral defining the scalar product (B1) extends upon the whole xy-plane and this erases the z-dependence.

To circumvent this difficulty, in this work we propose to define the scalar product in the space of functions $L_2(E)$ as

$$(f, g) = \int_E f^*(x, y, z)g(x, y, z) \, dx dy, \tag{41}$$

where the integration is now restricted to the domain E. With this definition, the scalar product (f, g) naturally becomes a function of z. Of course the definition (41) is to some extent arbitrary in that the choice of the integration domain E is partially discretionary (the only constraint is to be entirely contained within O). However, it is useful to remind here that the concepts themselves of "self-healing" and "minimum reconstruction distance" suffer from the same kind of arbitrariness. In other words, since both Eqs. (1) and (10) are impossible to satisfy over the *whole xy*-plane, one is forced to chose *where* these equations should be satisfied. A reasonable choice is to take E as the region bounded by the inner circle of radius $b \leq a$ in Fig. 1. However, different symmetries in the problem may dictate different choices, as we will explicitly show later in two examples.

Motivated by the introduction of the scalar product (41) and recalling that the distance $d(f, g)$ between two functions in $L_2(E)$ can be defined as $d(f, g) = \|f - g\|$, where $\|f\| = (f, f)^{1/2}$ [14], we found it convenient to introduce as z-dependent witness of self-healing, the function

$$w(z) = 1 - d_r, \tag{42}$$

where the *relative difference* d_r is defined as

$$
\begin{aligned}
d_r &= \frac{\|f - f_O\|}{\|f\| + \|f_O\|} \\
&= \frac{(f_A, f_A)^{1/2}}{(f, f)^{1/2} + [(f, f) - 2\operatorname{Re}(f, f_A) + (f_A, f_A)]^{1/2}}.
\end{aligned}
\tag{43}
$$

The limiting values of this witness function $w(z)$ are simply evaluated as follows. For a *totally opaque* obstacle, at $z = 0$ it must be $f_O = 0$ for all points $(x, y) \in E$. Therefore, from the definition (43) it follows that $w(0) = 0$. Vice versa, *if* for $z \geq z_0$ it has $f_O \approx \lambda_0 f$ for $(x, y) \in E$, then

$$w(z) \approx 1 - \left(\frac{1 - \lambda_0}{1 + \lambda_0}\right)^{1/2} \to 1 \qquad \text{for} \qquad \lambda_0 \to 1. \tag{44}$$

Therefore, we have

$$0 \leq w(z) \leq 1. \tag{45}$$

14

In the remainder of this section we will test the effectiveness of our witness function by using it to asses the self-healing ability of: *1.* the two-plane-wave "beam" described above, and *2.* a Gaussian beam.

1. Two-plane-wave beam

The two-plane-wave field (34) does not depend upon the variable y and has essentially a Cartesian geometry. Hence, we choose for E a square of side L centered at $(x = 0, y = 0)$, namely $E := \{(x, y) \in \mathbb{R}^2 : |x| \leq L \wedge |y| \leq L\}$. In this case the witness function $w(z)$ can be calculated analytically. However, the result of this calculation is very cumbersome and for the sake of clarity it will not be reported here. In Fig. 7 we display $w(z)$ as a function of z for different sizes of the square region E.
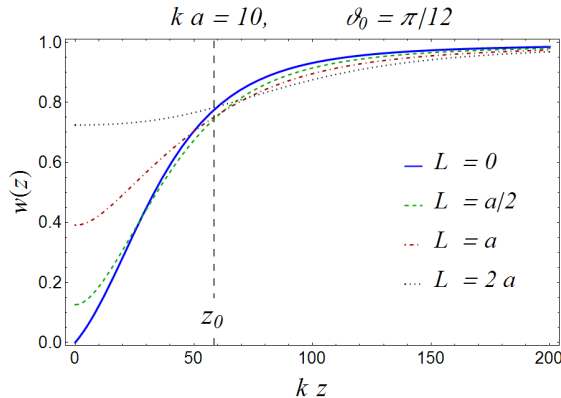

FIG. 7. Plot of the witness function $w(z)$ given in Eq. (42) evaluated for the two-plane-wave field (34) and the Gaussian obstruction (35) of width $ka = 10$ and centered at $x_0 = 0 = y_0$. The aperture of the "beam" is $\vartheta_0 = \pi/12$ and $z_0 \approx 58.5/k$ denotes the minimum reconstruction distance calculates as $z_0 = R(a)/\tan\theta$, where $R(a) = a\left[\ln\left(6 + 2^{5/2}\right)\right]^{1/2}$ denotes the half-width at half maximum of the intensity transmission function $|t_O(x, 0)|^2$. It is evident that when L increases, the dependence of $w(z)$ from z becomes weaker and weaker. The continuous blue line represents the asymptotic value of $w(z)$ achieved for $L/a \to 0$.

Since a soft-edge Gaussian obstacle has not a sharp boundary, we can shrink the region E to the single point $x = 0 = y$ and obtain the asymptotic value for the witness function represented by the continuous blue line in Fig. 7 and denoted with $\bar{w}(z)$.

The geometrical-optics value for the minimum reconstruction distance given in the literature, is obtained by calculating the point on the z-axis, namely the point at $x = 0 = y$, where the intensity of the obstructed field begin to raise from zero. Therefore, we can use the asymptotic form $\bar{w}(z)$, which is indeed calculated "on-axis", to estimate z_0 as follows. First, we choose a "threshold" value, say $\bar{w} = \Delta$, for the witness function. Then, we consider the beam as reconstructed only for those distances z from the obstruction such that $\bar{w}(z) \geq \Delta$.

15

By (numerically) inverting this relation we find the minimum reconstruction distance z_0 as

$$z_0 = \bar{w}^{-1}(\Delta). \tag{46}$$

The plots of $\bar{w}^{-1}(\Delta)$ as functions of either ϑ_0 and a are presented in Fig. 8 where they are compared with the geometrical-optics values.
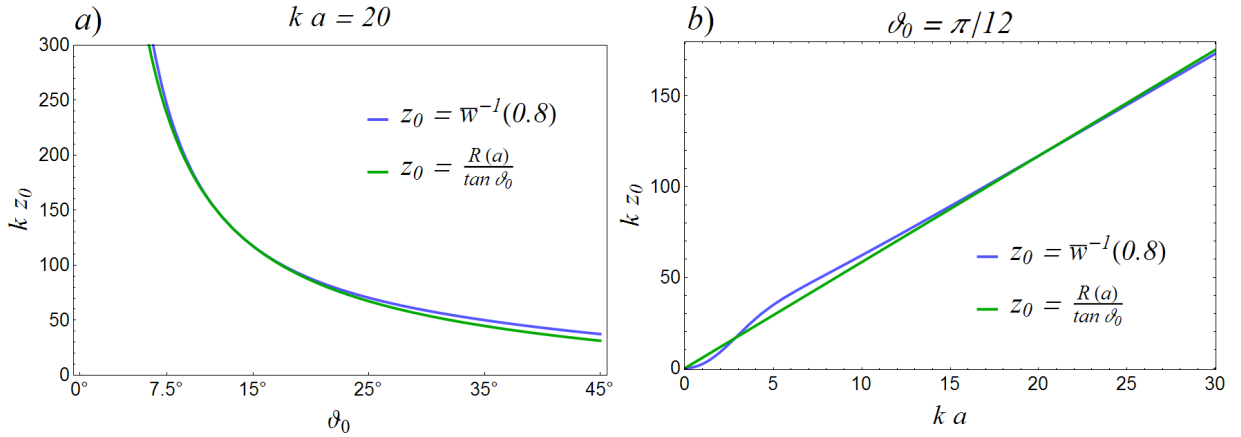

FIG. 8. Plots of $\bar{w}^{-1}(\Delta)$ in Eq. (46) as functions of either a) the aperture ϑ_0 and b) the width of the transmission function a. a) Plot of $\bar{w}^{-1}(\Delta)$ (blue line) as a function of ϑ_0, with $\Delta = 0.8$ and $ka = 20$. For comparison, the plot of the geometrical-optics value $z_0 = R(a)/\tan\theta$ (green line), is shown. b) Plot of $\bar{w}^{-1}(\Delta)$ (blue line) as a function of a, with $\Delta = 0.8$ and $\vartheta_0 = \pi/12$. For comparison, the plot of the geometrical-optics value $z_0 = R(a)/\tan\theta$ (green line), is shown.

In both cases the agreement between $\bar{w}^{-1}(\Delta)$ and the geometrical-optics value of z_0 is excellent.

2. Gaussian beam

The Gaussian beam studied in Sec. II C 1, whose field is given by Eq. (21), possess a cylindrical symmetry about the propagation axis z. Therefore, now we choose for E the disk of radius $b \leq a$ depicted in Fig. 1. Also in this case $w(z)$ can be calculated analytically. In Fig. 9a) we display $w(z)$ as a function of z for different values of b. When b goes to zero, we obtain the simple asymptotic form

$$\bar{w}(\zeta) = 1 - \frac{(1 + \zeta^2)^{1/2}}{\frac{\zeta}{2\alpha^2} + \left[1 + \frac{\zeta^2}{4\alpha^4}(1 + 2\alpha^2)^2\right]^{1/2}}, \tag{47}$$

16

where $\zeta = z/z_R$ and $\alpha = a/w_0$. It is interesting to notice that this function is "universal" in the sense that it does not depend explicitly on the angular spread θ_0 of the Gaussian beam. The plots of $\bar{w}(z)$ as function of z/z_R for different values of a/w_0, are presented in 9b). It is evident that when the size a of the obstruction goes to zero, the witness function tends to the unity.
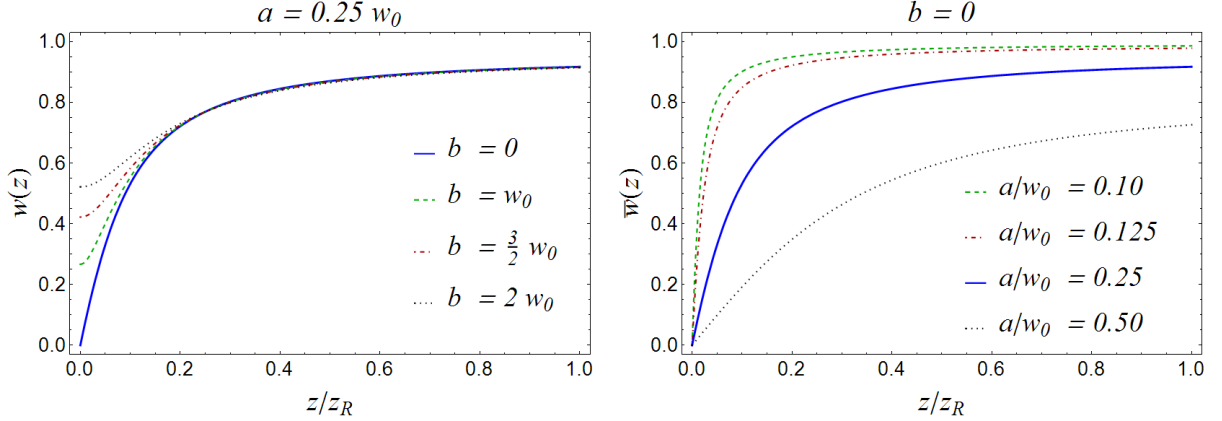

FIG. 9. a) Plots of the witness function $w(z)$ given in Eq. (42), evaluated for the Gaussian field (21) of waist w_0 and different radii b of the integration region E. It is evident that when b increases, the dependence of $w(z)$ from z becomes weaker. The continuous blue line represents the asymptotic value $\bar{w}(z)$ achieved for $b \to 0$. b) Plots of the asymptotic witness function $\bar{w}(z)$ (47) for several values of the width a of the soft-edge Gaussian obstruction. When the obstruction shrink to zero, then $\bar{w}(z) \to 1$, as expected from physical considerations.

In order to see the practical significance of $\bar{w}(z)$, in Fig. 10 next page we plot four sections of the unperturbed Gaussian beam (21) at different distances z from the obstacle, and we compare it with the obstructed beam profile. The witness function $\bar{w}(z)$ evidently provide for a quantitative estimation of the similarity between these two fields.

IV.   COMPARISON BETWEEN A GAUSSIAN BEAM AND A BESSEL BEAM

In this last section we compare a Gaussian with a Bessel beam both transmitted behind a soft-edge Gaussian obstruction and propagating in the *paraxial* regime. For comparison, we take the cone aperture ϑ_0 of the Bessel beam equal to the angular spread θ_0 of the Gaussian beam. In Figs. 11 and 12 we plot the intensity distributions (absolute value squared) evaluated at $y = 0$, of (left to right): the incident field, the "virtual" field transmitted by the aperture complementary to the obstruction, and the field transmitted behind the obstacle.
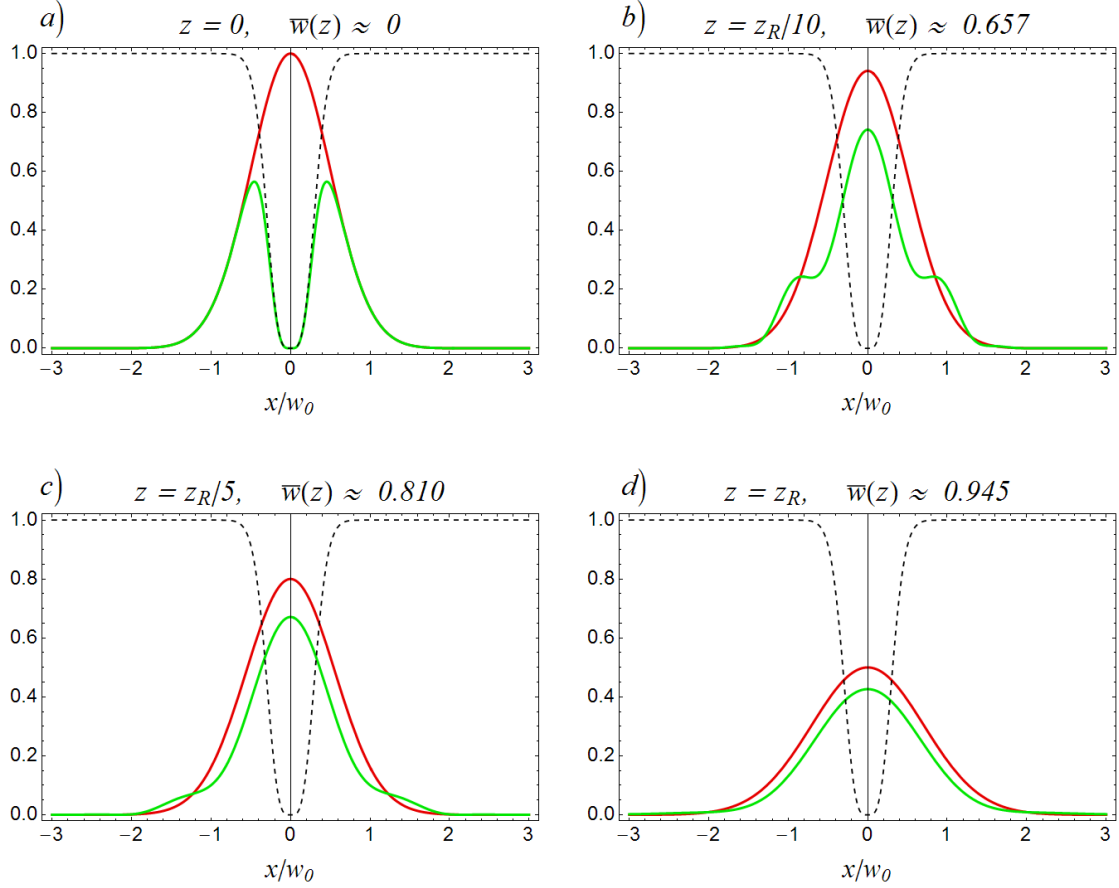
FIG. 10. Intensity distributions $I(x, y, z) = |g(x, y, z)|^2$ (red lines) and $I_O(x, y, z) = |g_O(x, y, z)|^2$ (green lines) evaluated at $y = 0$ and a) $z = 0$, b) $kz = 10$, c) $kz = 20$ and d) $kz = 40$. The black dashed curves represent the intensity transmission function $|t_O(x, y)|^2$ evaluated at $y = 0$. Here $\theta_0 = \pi/12$ and $a/w_0 = 0.2$.

Next, we plot the asymptotic witness functions $\bar{w}_G(z)$ and $\bar{w}_B(z)$ for the Gaussian and the Bessel beam, respectively. The witness function is defined by the values of the intensity on the z-axis according to the formula

$$\bar{w}(z) = 1 - \frac{\sqrt{I_A(z)}}{\sqrt{I(z)} + \sqrt{I_O(z)}}, \tag{48}$$

where $I_\#(z) = |f_\#(0, 0, z)|^2$. In Fig. 13 one can see that $\bar{w}_B(z) > \bar{w}_G(z)$ always, thus indicating a better self-healing property. The vertical line represents the geometrical-optics prediction for the minimum self-reconstruction distance $z_0/z_R \approx 0.312$, with

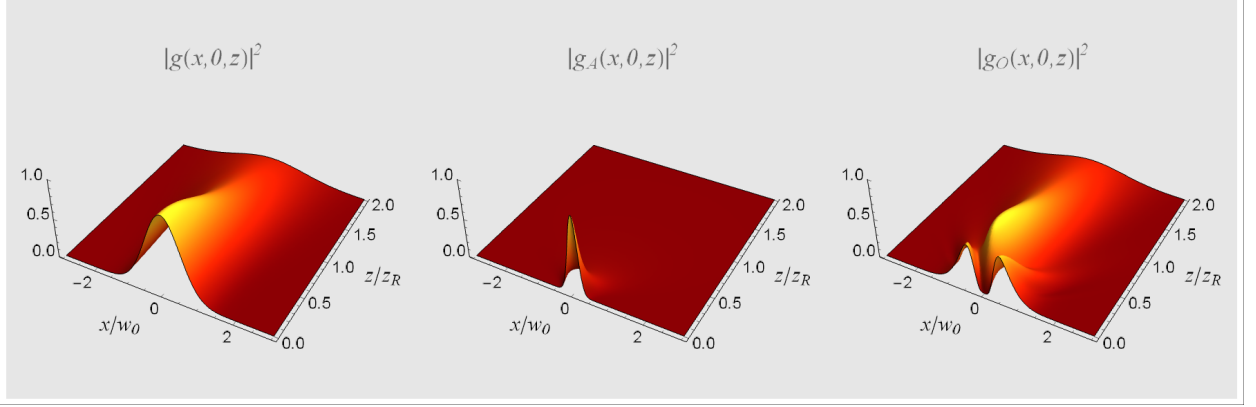$$\bar{w}_G(z_0) \approx 0.87, \qquad \bar{w}_B(z_0) \approx 0.90. \tag{49}$$

FIG. 11.　The plots are generated for a *Gaussian beam* with angular aperture $\theta_0 = 2/(kw_0) = \pi/32 \sim 6°$ and a soft-edge Gaussian obstruction with full width $a/w_0 = 0.2$ and $x_0 = 0 = y_0$.
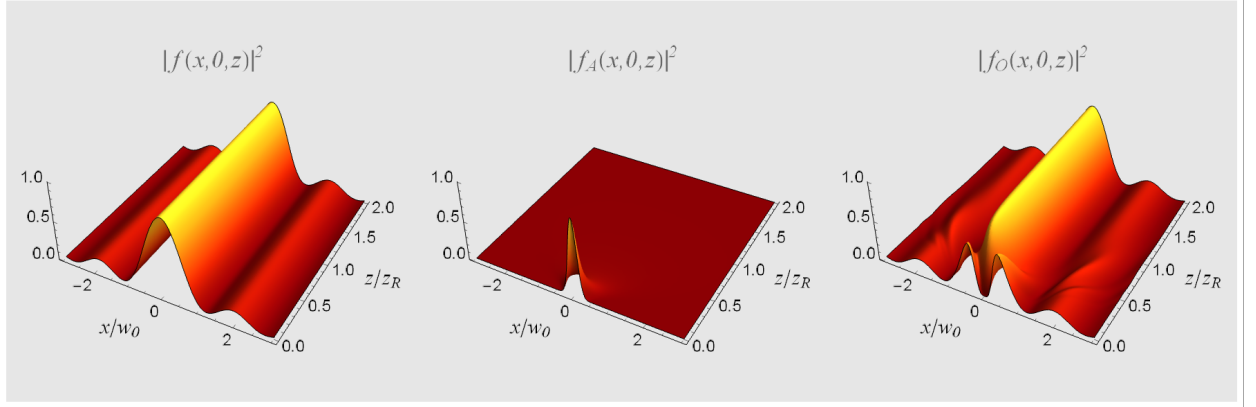

FIG. 12.　The plots are generated for a *Bessel beam* with cone aperture $\vartheta_0 = \pi/32 \sim 6°$ and a soft-edge Gaussian obstruction with full width $a/w_0 = 0.2$ and $x_0 = 0 = y_0$, where $w_0 = 2/(k\vartheta_0)$.

The two horizontal lines represent the "fidelity" values 0.9 and 0.95 such that

$$z_{0B} = \bar{w}_B^{-1}(0.9) \approx 0.298, \qquad z_{0B} = \bar{w}_B^{-1}(0.95) \approx 0.597, \qquad (50)$$
$$z_{0G} = \bar{w}_G^{-1}(0.9) \approx 0.413, \qquad z_{0G} = \bar{w}_G^{-1}(0.95) \approx 1.20. \qquad (51)$$

These results show that the Gauss beam reconstruct itself after the Bessel beam. Moreover, there is a limit to the reconstruction ability of a Gauss beam, because

$$\lim_{z/z_R \to \infty} \bar{w}_G(z) = \frac{1}{1 + \frac{a^2}{w_0^2}}, \qquad \lim_{z/z_R \to \infty} \bar{w}_B(z) = 1, \qquad (52)$$

so the fidelity for a Gaussian beam cannot reach the value 1. This is understandable because the Gauss beam has a finite energy which is partially lost because of the obstruction.
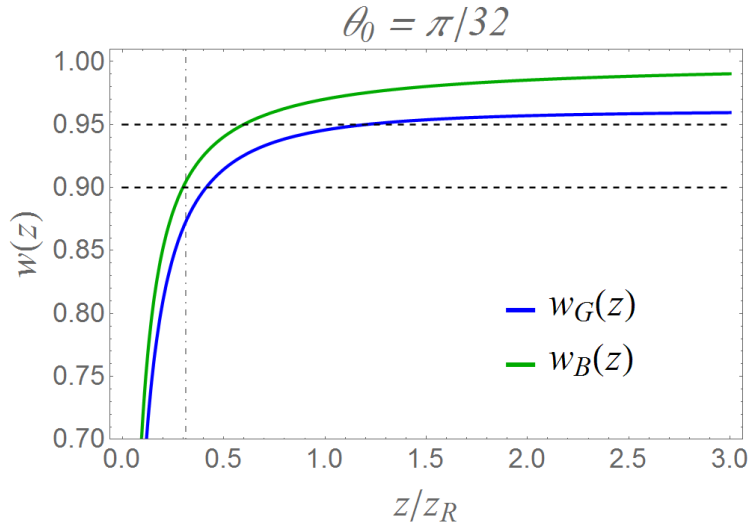
19

FIG. 13. The plots are generated for *Bessel* and *Gauss* beams with $\theta_0 = \vartheta_0 = \pi/32 \sim 6°$ and a soft-edge Gaussian obstruction with full width $a/w_0 = 0.2$ and $x_0 = 0 = y_0$, where $w_0 = 2/(k\theta_0)$.

V. CONCLUSIONS

In this work we studied and compared the self-healing properties of Gaussian, Bessel, Bessel-Gauss beams and of a pair of plane waves. We found a novel "universal" definition for the minimum reconstruction distance based on the angular spectrum distribution of a beam. Numerous examples are given in the text and illustrated with explanatory figures.

Appendix A: Notation

Three-dimensional vectors in either real and Fourier space are denoted with *Latin* letters: $\vec{r} = x\hat{x} + y\hat{y} + z\hat{z}$, $\vec{k} = k_x\hat{x} + k_y\hat{y} + k_z\hat{z}$. Two-dimensional vectors in either real and Fourier space are denoted with *Greek* letters: $\vec{\rho} = x\hat{x} + y\hat{y}$, $\vec{\kappa} = k_x\hat{x} + k_y\hat{y}$. Cylindrical coordinates in real and Fourier spaces are denoted with (ρ, ϕ, z) and (κ, φ, k_z), respectively, with $\rho^2 = x^2 + y^2$ and $\kappa^2 = k_x^2 + k_y^2$. All fields considered here are monochromatic with wave number k and angular frequency $\omega = ck$.

The *Fourier transform* of a function $g(x, y)$ of two independent variables x and y will be denoted either by $\mathcal{F}[g](k_x, k_y)$ or by $G(k_x, k_y)$ and is defined by

$$G(k_x, k_y) = \frac{1}{2\pi} \iint\limits_{-\infty}^{\infty} g(x, y) \exp\left[-i\left(xk_x + yk_y\right)\right] dxdy. \tag{A1}$$

Similarly, the *inverse Fourier transform* of a function $G(k_x, k_y)$ will be represented either

20

by $\mathcal{F}^{-1}[G](x,y)$ or by $g(x,y)$ and is defined as

$$g(x,y) = \frac{1}{2\pi} \int\!\!\!\int\limits_{-\infty}^{\infty} G(k_x, k_y) \exp\left[i\left(xk_x + yk_y\right)\right] dk_x dk_y. \tag{A2}$$

The two-dimensional Dirac delta symbol $\delta(\vec{\kappa} - \vec{\kappa}')$ stands for

$$\delta(\vec{\kappa} - \vec{\kappa}') = \delta(k_x - k_x')\delta(k_y - k_y'), \tag{A3}$$

and is defined as

$$\delta(\vec{\kappa} - \vec{\kappa}') = \frac{1}{(2\pi)^2} \int\!\!\!\int\limits_{-\infty}^{\infty} \exp\left[ix\left(k_x - k_x'\right)\right] \exp\left[iy\left(k_y - k_y'\right)\right] dxdy. \tag{A4}$$

Appendix B: The Chu&Wen proposal

In the article [9], Chu&Wen defined the scalar product in the space of functions $L_2(\mathbb{R}^2)$ as

$$\langle f, g \rangle = \int\!\!\!\int\limits_{-\infty}^{\infty} f^*(x,y,z)g(x,y,z)\,dxdy. \tag{B1}$$

Later, in their equation (1), they proposed the following measure of the similarity between two given functions f and g:

$$\text{Similarity} \sim \cos\left(f \cdot g\right) = \frac{\langle f, g \rangle}{\|f\|\,\|g\|}, \tag{B2}$$

where the *norm* of a function is defined as $\|f\| = \langle f, f \rangle^{1/2}$. This notation may seems not very appropriate because the right side of Eq. (B2) can be a complex number. A more suitable definition yielding to a non-negative number is simply

$$\text{Similarity} \sim \frac{|\langle f, g \rangle|}{\|f\|\,\|g\|}, \tag{B3}$$

which coincides with the standard definition of *fidelity of quantum pure states* in quantum mechanics [15].

Using the Parseval's theorem, Chu&Wen were able to show that the similarity defined as in Eq. (B2) cannot depend upon the propagation distance z (in their derivation Chu&Wen implicitly assumed that the considered angular spectrum did not contain evanescent waves). Therefore, they adopted a new description of similarity, given in their equation (11), defined as

$$\text{Similarity} \sim \cos\left(|f| \cdot |g|\right) = \frac{\langle |f|, |g| \rangle}{\|f\|\,\|g\|}. \tag{B4}$$

With this definition, the similarity between f and g becomes a function of the propagation distance z. However, if one applies Eq. (B4) to pure (namely, non Gaussian) Bessel beams, this similarity function becomes z-independent. Therefore, also the definition (B4) in some circumstances may be not fully satisfactory.

[1] D. McGloin, and K. Dholakia, "Bessel beams: Diffraction in a new light," Contemporary Physics **46**,15-28 (2005).

[2] R. Jáuregui and S. Hacyan, "Quantum-mechanical properties of Bessel beams," Phys. Rev. Lett. **71**, 033411 (2005).

[3] J. Arlt,V. Garces-Chavez, W. Sibbett, and K. Dholakia, "Optical micromanipulation using a Bessel light beam," Opt. Commun. **197**, 239-245 (2001).

[4] V. Garcés-Chávez, D. McGloin, H. Melville, W. Sibbett, and K. Dholakia, "Simultaneous micromanipulation in multiple planes using a self-reconstructing light beam," Nature **419**, 145-147 (2002).

[5] F. O. Fahrbach, P. Simon, and A. Rohrbach, "Microscopy with self-reconstructing beams," Nat. Phot. **4**, 780-785 (2010).

[6] F. O. Fahrbach, and A. Rohrbach, "Propagation stability of self-reconstructing Bessel beams enables contrast-enhanced imaging in thick media," Nat. Commun. 3:632 doi: 10.1038/ncomms1646 (2012).

[7] M. McLaren, T. Mhlanga, M. J. Padgett, F. S. Roux, and Andrew Forbes, "Self-healing of quantum entanglement after an obstruction," Nat. Commun. 5:3248 doi: 10.1038/ncomms4248 (2014).

[8] X. Chu, "Analytical study on the self-healing property of Bessel beam," Eur. Phys. J. D **66**, 259 (2012).

[9] X. Chu, and W. Wen, "Quantitative description of the self-healing ability of a beam," Opt. Exp. **22**, 6899-6904 (2012).

[10] A. Aiello, and G. S. Agarwal, "Wave-optics description of self-healing mechanism in Bessel beams," Opt. Lett. **39**, 6819 (2014).

[11] E. W. Weisstein, "Integral Equation." From MathWorld–A Wolfram Web Resource. `http://mathworld.wolfram.com/IntegralEquation.html`

[12] L. Mandel and E. Wolf, *Optical Coherence and Quantum Optics*, (Cambridge University Press, 1995).

[13] I. S. Gradshteyn and I. M. Ryzhik, *Table of Integrals, Series, and Products*, 5th ed., Academic Press (1994).

[14] A. N. Kolmogorov and S. V. Fomin, *Elements of the theory of functions and functional analysis*, Dover Publications, Inc. (1999).

[15] M. A. Nielsen and I. L. Chuang, "Quantum Computation and Quantum Information," Cam-

bridge University Press (2000).